Schweizer Archiv für Tierheilkunde
S. Ohlerth et al., Band 156, Heft 10, Oktober 2014, 489–497
DOI 10.1024/0036-7281/a000636

Computed tomography of the thorax in calves from birth to 105 days of age

S. Ohlerth[1], H. Augsburger[2], M. Abé[3], S. Ringer[4], L. Hatz[4], U. Braun[3]

[1]Division of Diagnostic Imaging, [2]Institute of Veterinary Anatomy, [3]Department of Farm Animals and [4]Division of Anaesthesiology, Vetsuisse Faculty, University of Zurich

Summary

The present study was undertaken to provide computed tomographic (CT) reference values for structures in the thorax of the calf. Six clinically healthy Holstein-Friesian calves were anaesthetized. Transverse pre- and postcontrast images with a reconstructed 1.5-mm slice thickness were obtained using a multislice-CT scanner at 6 different time points from birth to 105 days of age. Absolute and relative measurements of the trachea, heart, cranial and caudal vena cava, thoracic aorta, right and left principal bronchi, right and left caudal lobar bronchi and the accompanying branches of the right and left pulmonary artery and vein, thoracic lymph nodes and lung density were taken for every time point. All animals were euthanized after the last CT scan, and 4 calves were frozen to generate an atlas comparing gross anatomy with CT. During the study, 4 animals temporarily showed coughing and mucopurulent nasal discharge, and mild to moderate bronchopneumonia and pleuritis were diagnosed using CT. Animals recovered with treatment; however, mild to moderate CT changes remained throughout the study. Even in the 2 clinically normal animals, mild bronchopneumonia was diagnosed on CT.

Keywords: computed tomography, angiography, calf, thorax, bronchopneumonia

Computertomographie des Thorax von Kälbern von der Geburt bis zum Alter von 105 Tagen

In dieser Arbeit wurden computertomographische (CT) Normalwerte für Strukturen des Thorax beim Kalb erhoben. Sechs klinisch gesunde Holstein-Friesian-Kälber wurden dafür in Vollnarkose von der Geburt bis zum Alter von 105 Tagen 6 mal mit einem Mehrschicht-Computertomographen nativ und angiographisch untersucht. Es wurden Bilder mit einer Schichtdicke von 1.5 mm rekonstruiert. Absolute und relative Messungen des Herzens, der Trachea, Aorta thoracica, Vena cava cranialis und caudalis, Bronchi principales, Bronchi lobares caudales mit den Ästen der Arteriae und Venae pulmonales, Lymphknoten und Lungendichte wurden zu jedem Zeitpunkt ausgeführt. Alle Tiere wurden im Anschluss an die letzte Untersuchung euthanasiert, und 4 Kälber wurden für eine vergleichende Gegenüberstellung der CT Bilder mit anatomischen Schnittbildern tiefgefroren. Während der Studie entwickelten 4 Kälber Husten und Nasenausfluss. Mittels CT wurden eine leicht- bis mittelgradige Bronchopneumonie und Pleuritis diagnostiziert. Obwohl sich die Tiere nach Behandlung vollständig erholten, persistierten leicht- bis mittelgradige CT Veränderungen bis zum Ende der Studie. Selbst bei den beiden klinisch gesunden Tieren wurde im CT eine leichtgradige Bronchopneumonie diagnostiziert.

Schlüsselwörter: Computertomographie, Angiographie, Kalb, Thorax, Bronchopneumonie

Introduction

Computed tomography (CT) represents a highly reliable, non-invasive technique for the evaluation of thoracic structures and is considered the gold standard for evaluation of lung diseases in humans (Collins, 2001). Although CT examination is expensive, the use of this technology in veterinary medicine has become fairly widespread. Examination times using multi-slice CT are relatively short, which means that thoracic scans can be obtained easily and quickly in anaesthetized animals. The diagnostic usefulness of CT in pulmonary diseases has been studied in dogs, cats, goats and calves (Johnson et al., 2004, 2005; Lubbers et al., 2007; Ohlerth et al., 2012; Armbrust et al., 2012). Diseases of the respiratory tract are common in calves and often occur as a herd problem. There are no reports of CT reference values for structures of the normal thorax in calves. The purpose of the present study was to use CT to investigate the normal thoracic structures in calves from birth to 105 days of age.

Animals, Material and Methods

Animals

Six Holstein-Friesian bull calves were used. They ranged in age from birth to 2 days (mean ± sd, 1.5 ± 0.55 days) and weighed 33.5 to 55.0 kg (47.8 ± 8.0 kg) at the time of the first examination. They were determined to be healthy based on the clinical examination, laboratory analyses and echocardiography. BVDV-antigen testing was negative.

CT examination

Each calf underwent six CT examinations 21 days apart (scan 1 – scan 6) using a 40-slice CT scanner (Somatom Sensation Open, Siemens AG, Zurich). Animals were not fasted before general anaesthesia, which was induced with midazolam (Dormicum®, 0.3 mg/kg) and ketamine (Narketan®, 3 mg/kg) and maintained with 2 – 2.5 % isoflurane (Forene®) delivered in oxygen through an endotracheal tube. Calves were positioned in sternal recumbency using a foam trough.

After a native scan of the thorax, an iodinated contrast medium (Ultravist®-370) was given intravenously at a dose of 2 ml/kg BW via a power injector. The flow rate was adjusted to the scan time and calculated as follows: flow rate (ml/s) = total contrast volume (ml)/(scan time + 10 s) (Makara, 2011). The maximum injection rate and total volume were defined as 6 ml/s and 200 ml, respectively. Bolus tracking in the pulmonary outflow tract with a threshold of 100 Hounsfield Units (HU) was used to start CT-angiography during a single breath-hold technique. Images were acquired from the thoracic inlet to the cranial abdomen with 3 mm slice thickness, an increment of 2.5 mm and a pitch of 1.2, 120 kVp and 200 mA. Data were reconstructed with a soft tissue, bone and lung algorithm to images with 1.5 mm slice thickness. Image interpretation and measurements were done with dedicated software in transverse, sagittal, dorsal or oblique planes (OsiriX Open Source™ 5.0.2, OsiriX Foundation, Geneva). Cardiovascular structures were assessed on the angiographic images. Bony structures, soft tissues and the lung were evaluated in a bone (window width [WW] 3000 HU, window level [WL] 300 HU), soft tissue (WW 400 HU, WL 40 HU) and lung window (WW 1200 HU, WL – 600 HU), respectively.

In the bone window, the height of the thorax was measured in the transverse plane between the ventral aspect of the first thoracic vertebra (T1) and the manubrium and between T4 and T8 and the corpus sterni, respectively. The width of the thorax was measured as the maximum horizontal distance between the rib cage at the level of T1, T4 and T8. The angle between the dorsal wall of the trachea and the spine was determined in the median plane. The length of the thoracic vertebra at the level of the tracheal bifurcation was measured along its ventral surface.

In the soft-tissue window, the short axis of the heart was measured in the sagittal plane at the level of the atrioventricular valves. Perpendicular to the short axis, the long axis of the heart was measured from the ventral border of the tracheal bifurcation to the cardiac apex. The long and short axis dimensions were added; the sum was transposed onto the vertebral column and recorded as the number of vertebrae (vertebral heart score, VHS) beginning at the cranial edge of T4. In the sagittal plane, the maximal height of the cranial and caudal venae cavae and the thoracic aorta was measured along their course.

In the lung window, the maximal height and width of the lumen of the trachea were measured at the level of the thoracic inlet. The cross-sectional area of the lumen of the trachea was measured at the thoracic inlet and just cranial to its bifurcation. Just caudal to the tracheal bifurcation, the inner and outer cross-sectional areas of the right and left principal bronchi were evaluated. The difference between the outer and inner cross-sectional areas was defined as the wall area.

Lung density (Hounsfield units, HU) was determined on the native images in a defined 2-cm^2 area at the level of the caudal lobar bronchi in the periphery of the right and left lung parenchyma. At the level of T7 to T8, the inner cross-sectional area of the caudal lobar bronchus and the cross-sectional area of the accompanying branches of the pulmonary artery and vein were calculated on the right and left. In the dorsal plane, the angle between the midaxis of both principal bronchi was assessed. Lung changes were classified according to a system described for the assessment of high resolution CT findings in the dog (Johnson, 2004). This classification system represents a modified method used for humans (Collins, 2001).

The calves were euthanized after the last CT scan at the age of 105 days while still under anaesthesia. While 2 animals went for necropsy, 4 calves were frozen and later cut into slices in different planes for comparison with the digital CT images.

Descriptive statistics were calculated using the SPSS statistics program (Version 19, IBM Corporation, Armonk, New York). The Wilk Shapiro test was used to test continuous variables for normality. Differences between measurements with a normal distribution of the first and the five subsequent examinations were analyzed by means of a two-tailed paired t-test, and the Wilcoxon rank test was used for measurements with non-normal distribution. Changes in variables over time were examined using analysis of variance for repeated measures or a repeated measures general linear model (STATA©12, StataCorp LP, Collage Station, Texas). A P value ≤ 0.05 was considered significant.

This study was authorized by the veterinary office of the Canton of Zurich (permit number 18/2010).

Results

Clinically, 4 of the 6 calves temporarily developed mild to moderate bronchopneumonia accompanied by coughing and mucopurulent nasal discharge, from which they recovered clinically after antibiotic treatment. One of these 4 calves underwent postmortem examination after the last CT scan and a diagnosis of moderate diffuse purulent bronchopneumonia was made. The second calf that underwent necropsy was always healthy during the study and had normal postmortem findings.

All structures seen in the CT images were easily identified with the help of the anatomical cadaver slices. The comparison of soft-tissue and lung windows with transverse anatomical slices at the level of each vertebra from T2 to T11 was published elsewhere (Abé, 2013). The basic structure of the thoracic organs and the course of blood vessels in the soft tissue window were in agreement with anatomy textbooks (Schummer and Habermehl, 1996; Waibl and Wilkens, 1996 a, b). During the study period, the thoracic organs changed mostly in size and sometimes slightly in location. The descriptive statistics relating to the thoracic organs are listed in Table 1.

Mean thoracic height and width increased from cranial to caudal, and all three vertical measurements, as well as the length of the thoracic vertebra at the level of the bifurcation of the trachea, increased from scan 1 to scan 6. During the first few days of life, the heart extended from the level of T3 to the level of T8 and its long axis was tilted moderately cranially. At the time of the last scan, the heart extended from T2 to T7 with a much less pronounced cranial tilt of the long axis of the heart (Fig. 1). Absolute measurements of height and width of the heart increased significantly until CT scan 4 and 3, respectively, whereas the vertebral heart score decreased significantly until the CT scan 5. The maximal heights of the aorta and cranial vena cava also increased progressively until the CT scan 3 and 4, respectively, but the maximal height of the caudal vena cava changed little during the study period. The ratio of the maximal height of the caudal vena cava to the maximal height of the aorta and the ratio of the maximal height of the caudal vena cava to the length of the thoracic vertebra at the level of the bifurcation of the trachea decreased significantly from scan 1 to scan 2 but changed little during the remainder of the study period.

The unpaired left thoracic part of the thymus was seen on the left side in the precardial mediastinum at all scans (Fig. 2). In contrast, the *isthmus cervicothoracalis* and the caudal unpaired apex of the cervical part were not clearly delineated from the surrounding structures. In the sagittal plane, the unpaired left thoracic part appeared in all scans as a triangular to trapezoid structure lateroventral to the brachiocephalic trunk and to the left of the cranial vena cava. Assessed subjectively, the size of the unpaired left thoracic part of the thymus decreased only marginally during the study period.

Three of the constant lymph nodes could be identified in all calves at all 6 scans. One cranial mediastinal lymph node was located on the right side of the cranial mediastinum next to the trachea. The largest of the middle mediastinal lymph nodes was located dorsal to the base of the heart on the right and was seen in the sagittal plane in the angle between the aorta and oesophagus. The large and elongated caudal mediastinal lymph node was situated further caudally between the aorta and oesophagus and in two calves was divided in two. The relatively small cranial sternal lymph node was identified as a paired lymph node at all scans in 5 calves. Of the caudal sternal lymph nodes, only one could be accurately identified and it was located dorsally on the transverse thoracic muscle. The left tracheobronchial lymph node was seen in all calves between the bifurcation of the trachea and pulmonary trunk from scan 2 onward, but differentiating it from surrounding structures was difficult. The tiny intercostal lymph nodes, the thoracic aortic lymph nodes and the cranial tracheobronchial lymph nodes were not seen in any of the calves. The right tracheobronchial lymph node was the only inconstant lymph node that could be accurately identified in three calves from scan 3 onward. With the exception of the medial lobe of the right lung, all lung lobes could be identified at all scans based on the delicate, regular, soft-tissue-dense pleural fissures. At scan 1, the bifurcation of the trachea was at the level of T5 in all calves, and at the last scan, it was at the level of T4.

The mean height, width and cross-sectional area of the trachea at the thoracic inlet and at the level of the bifurcation increased slightly during the study period but the mean ratio of tracheal height to thoracic height did not change significantly. The size of the two main bronchi (inner and outer cross-sectional areas and wall area) and the angle between them increased continuously during the study period, whereas the inner cross-sectional area of both main bronchi at the level of T7 to T8 decreased from scan 1 to scan 2 and then gradually increased.

At all scans, the branches of the pulmonary artery were seen immediately adjacent and lateral to the corresponding lobar bronchi and the branches of the pulmonary vein were seen immediately adjacent and medial to the corresponding lobar bronchi. This was characteristic of lung type I (McLaughlin et al., 1961), and their diameter changed little during the study. The mean density of the right and left caudal lung lobes did not change significantly during the study (–700 to –624 HU). The right lung was always larger than the left lung in the transverse plane.

On the CT scan 1, mild or moderate (with pleuritis) bronchopneumonia was diagnosed in 4 animals and 1 calf, respectively. Only one animal was considered normal on CT initially; however, it was one of the 4 animals developing clinical bronchopneumonia. All 4 calves that temporarily developed clinical signs of bronchopneumonia, showed moderate bronchopneumonia and/or pleuritis in CT at one time point at the least. After successful treatment and until the end of the study, these animals were clini-

Table 1: Descriptive statistics of thoracic measurements in 6 clinically normal calves of 6 consecutive CT examinations 3 weeks apart [mean, standard deviation (minimum-maximum)]; CSA: cross-sectional area; *first measurement which was significantly different from first CT scan: $p < 0.05$).

Variable	CT scan					
	Scan 1 (1–2 days old)	Scan 2 (21 days old)	Scan 3 (42 days old)	Scan 4 (63 days old)	Scan 5 (84 days old)	Scan 6 (105 days old)
Thoracic height at T1 (cm)	11.5, 0.78 (10.5–12.6)	12.2, 0.47 (11.5–12.8)	13.2, 0.87 (11.9–13.9)*	13.9, 1.0 (12.5–15.5)	14.5, 1.2 (12.5–15.8)	15.8, 1.6 (13.4–18.4)
Thoracic height at T4 (cm)	14.8, 1.53 (12.7–16.9)	16.9, 0.89 (15.3–17.8)*	19.1, 1.36 (16.8–20.4)	19.5, 0.79 (19.1–21.3)	20.7, 1.33 (18.3–21.9)	21.7, 1.07 (19.9–22.7)
Thoracic height at T8 (cm)	16.0, 1.33 (14.1–17.5)	18.2, 1.06 (17.2–19.7)*	20.5, 0.6 (19.6–21.1)	21.2, 0.89 (20.2–22.0)	23.1, 0.66 (22.7–23.6)	23.4, 0.32 (23.2–23.7)
Thoracic width at T1 (cm)	6.0, 0.44 (5.3–6.4)	6.1, 0.43 (5.2–6.4)	6.7, 0.43 (5.9–7.0)*	7.1, 0.47 (6.3–7.5)	7.3, 0.53 (6.4–7.8)	7.4, 1.04 (6.2–9.4)
Thoracic width at T4 (cm)	9.9, 0.65 (9.2–10.7)	11.1, 0.38 (10.5–11.6)*	12.9, 2.06 (10.7–16.3)	13.6, 1.28 (12.0–15.0)	15.6, 2.84 (12.3–18.9)	18.4, 3.8 (13.8–22.2)
Thoracic width at T8 (cm)	12.9, 1.02 (11.3–14.2)	15.0, 0.77 (14.1–15.9)*	17.9, 1.41 (16.1–19.8)	20.8, 2.65 (18.3–25.3)	27.2, 6.21 (19.6–36.9)	29.7, 5.21 (24.6–35.9)
Cardiac width (cm)	9.7, 0.83 (9.1–11.2)	10.9, 0.74 (9.6–11.8)*	11.8, 0.37 (11.3–12.3)	12.2, 0.62 (11.2–12.9)	12.0, 1.21 (10.0–13.6)	12.6, 0.44 (12.2–13.4)
Cardiac height (cm)	14.4, 0.91 (13.6–16.1)	15.1, 0.67 (13.9–16.0)	15.3, 0.59 (14.2–15.9)	16.7, 1.65 (13.9–18.9)*	15.9, 1.16 (14.4–17.3)	17.2, 0.58 (16.1–17.7)
Vertebral heart score (VHS)	9.3, 0.3 (9.0–10.0)	9.3, 0.24 (9.0–9.5)	9.1, 0.21 (9.0–9.5)	8.8, 0.22 (8.5–9.0)*	7.9, 0.49 (7.5–9.0)	8.2, 0.27 (8.0–9.0)
Maximal height of aorta (cm)	1.7, 0.21 (1.4–2.0)	2.0, 0.19 (1.7–2.2)*	2.1, 0.1 (2.0–2.3)	2.4, 0.22 (2.0–2.6)	2.6, 0.26 (2.2–2.9)	2.7, 0.31 (2.4–3.2)
Maximal height of cranial vena cava (cm)	1.7, 0.21 (1.75–2.0)	1.9, 0.24 (1.5–2.2)	2.1, 0.21 (1.7–2.3)*	2.2, 0.22 (1.0–2.5)	2.3, 0.34 (1.7–2.6)	2.3, 0.28 (1.8–2.6)
Maximal height of caudal vena cava (cm)	2.0, 0.27 (1.7–2.5)	1.8, 0.42 (1.4–2.4)	1.8, 0.12 (1.6–2.0)	2.1, 0.2 (1.2–2.5)	1.8, 0.27 (1.4–2.1)	2.0, 0.25 (1.7–2.4)
Maximal height of caudal vena cava/aorta	1.2, 0.14 (1.0–1.4)	0.9, 0.18 (0.7–1.2)*	0.8, 0.07 (0.7–0.9)	0.9, 0.24 (0.5–1.2)	0.7, 0.08 (0.6–0.8)	0.8, 0.15 (0.5–0.9)
Maximal height of caudal vena cava/length of vertebra at the level of the bifurcation of the trachea	0.8, 0.11 (0.7–1.0)	0.7, 0.15 (0.5–0.9)*	0.6, 0.06 (0.6–0.7)	0.6, 0.14 (0.4–0.8)	0.5, 0.09 (0.4–0.6)	0.6, 0.09 (0.5–0.7)
Tracheal height at thoracic inlet (cm)	2.0, 0.22 (1.8–2.4)	2.3, 0.32 (1.9–2.7)	2.3, 0.27 (1.9–2.6)	2.3, 0.32 (1.9–2.8)	2.3, 0.33 (1.8–2.7)	2.7, 0.33 (2.3–3.3)*
Tracheal width at thoracic inlet (cm)	2.0, 0.19 (1.7–2.2)	2.0, 0.21 (1.8–2.4)	2.1, 0.08 (2.0–2.2)	2.1, 0.25 (1.6–2.3)	2.0, 0.17 (1.8–2.3)	2.4, 0.26 (2.1–2.7)*
CSA of trachea at thoracic inlet (cm^2)	3.3, 0.48 (2.7–4.2)	3.9, 0.81 (3.1–5.4)	4.0, 0.79 (2.8–5.0)	4.0, 0.99 (2.6–5.3)	3.7, 1.28 (2.4–5.4)	5.3, 1.3 (3.6–7.5)*
CSA of trachea at bifurcation (cm^2)	3.1, 0.79 (2.1–4.4)	3.7, 0.92 (2.4–5.2)	3.8, 0.62 (3.1–4.6)	4.0, 0.59 (3.4–5.0)*	4.2, 0.82 (3.5–5.7)	5.3, 1.5 (4.0–8.0)
Tracheal height/thoracic height at thoracic inlet	0.18, 0.01 (0.17–0.19)	0.19, 0.02 (0.17–0.22)	0.18, 0.02 (0.13–0.19)	0.16, 0.02 (0.12–0.19)	0.16, 0.02 (0.12–0.18)	0.17, 0.02 (0.14–0.19)
Outer CSA of right principal bronchus (cm^2)	1.8, 0.4 (1.4–2.3)	2.6, 0.5 (2.0–3.5)*	2.9, 0.42 (2.9–4.2)	3.7, 0.71 (2.7–4.6)	4.0, 0.49 (3.2–4.5)	4.3, 0.89 (3.5–6.0)
Inner CSA of right principal bronchus (cm^2)	1.2, 0.29 (0.8–1.5)	1.5, 0.38 (1.2–2.2)	2.0, 0.41 (1.6–2.7)*	1.9, 0.45 (1.2–2.4)	2.2, 0.32 (1.6–2.6)	2.3, 0.72 (1.6–3.7)
CSA of wall of right principal bronchus (cm^2)	0.6, 0.11 (0.5–0.8)	1.1, 0.26 (0.7–1.5)*	1.4, 0.09 (1.3–1.5)	1.7, 0.3 (1.3–2.2)	1.8, 0.29 (1.5–2.3)	2.0, 0.37 (1.5–2.4)
Outer CSA of left principal bronchus (cm^2)	1.7, 0.39 (1.3–2.3)	2.4, 0.7 (1.9–3.8)	3.3, 0.8 (2.3–4.3)*	3.1, 0.72 (2.2–4.3)	3.9, 0.69 (3.0–4.6)	4.0, 1.16 (2.6–5.7)
Inner CSA of left principal bronchus (cm^2)	1.1, 0.26 (0.81–1.4)	1.5, 0.5 (1.0–2.7)	1.9, 0.5 (1.3–2.7)*	1.7, 0.43 (1.0–2.2)	2.2, 0.5 (1.1–2.6)	2.2, 0.68 (1.6–3.8)
CSA of wall of left principal bronchus (cm^2)	0.6, 0.16 (0.4–0.9)	0.8, 0,18 (0.6–1.1)*	1.3, 0.36 (0.9–1.8)	1.4, 0.3 (1.2–2.1)	1.9, 0.35 (1.3–2.1)	1.7, 0.49 (0.94–2.2)
Interbronchial angle (°)	41.1, 3.6 (36.1–46.5)	42.0, 4.7 (35.2–47.4)	47.7, 7.9 (37.8–61.1)	49.2, 7.0 (38.3–58.6)*	58.0, 12.6 (41.2–75.6)	63.7, 8.7 (51.2–73.3)
Inner CSA of left caudal lobar bronchus (cm^2)	0.6, 0.14 (0.4–0.8)	0.3, 0.09 (0.2–0.4)*	0.4, 0.17 (0.1–0.6)	0.4, 0.09 (0.3–0.5)	0.4, 0.16 (0.2–0.6)	0.5, 0.15 (0.3–0.8)

Table 1: Descriptive statistics of thoracic measurements in 6 clinically normal calves of 6 consecutive CT examinations 3 weeks apart [mean, standard deviation (minimum-maximum)]; CSA: cross-sectional area; *first measurement which was significantly different from first CT scan: $p < 0.05$). (continuation)

Variable	CT scan					
	Scan 1 (1–2 days old)	Scan 2 (21 days old)	Scan 3 (42 days old)	Scan 4 (63 days old)	Scan 5 (84 days old)	Scan 6 (105 days old)
CSA of caudal lobar branch of left pulmonary vein (cm^2)	0.6, 0.21 (0.3–1.0)	0.3, 0.06 (0.2–0.4)*	0.5, 0.15 (0.2–0.7)	0.5, 0.15 (0.3–0.7)	0.5, 0.28 (0.2–0.9)	0.6, 0.15 (0.4–0.7)
Inner CSA of right caudal lobar bronchus (cm^2)	0.7, 0.14 (0.5–0.8)	0.3, 0.14 (0.2–0.5)*	0.4, 0.2 (0.2–0.7)	0.4, 0.11 (0.2–0.5)	0.5, 0.16 (0.2–0.7)	0.5, 0.2 (0.3–0.8)
CSA of caudal lobar branch of right pulmonary artery (cm^2)	0.7, 0.23 (0.5–1.1)	0.4, 0.26 (0.2–0.9)*	0.5, 0.21 (0.3–0.8)	0.5, 0.13 (0.4–0.7)	0.5, 0.13 (0.4–0.7)	0.7, 0.16 (0.4–0.8)
CSA of caudal lobar branch of right pulmonary vein (cm^2)	0.7, 0.13 (0.5–0.9)	0.5, 0.4 (0.2–1.4)*	0.5, 0.22 (0.3–0.7)	0.5, 0.2 (0.3–0.7)	0.5, 0.21 (0.3–0.9)	0.7, 0.3 (0.3–1.0)

cally normal; however, in CT scan 6, mild or moderate bronchopneumonia was still apparent in 2 animals each (1 animal with additional pleuritis). Also, in the 2 calves, which were clinically normal throughout the study, mild bronchopneumonia with pleuritis was seen throughout the study until the last CT scan. The following CT changes were consistently seen in all calves: mild to moderate consolidation of the ventral region of the cranial and caudal lung lobes, mild to severe ground glass opacity, mild to moderate bronchiectasis and peribronchovascular thick-

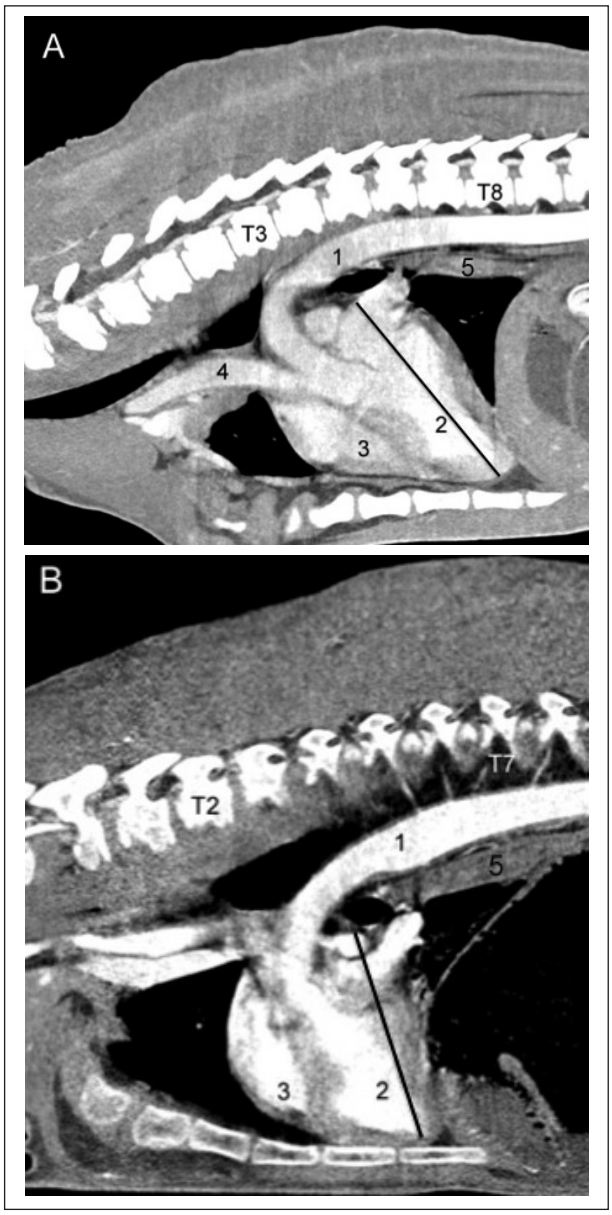

Figure 1: Sagittal CT angiographic images of the thorax of a calf. At the age of 1 day (A), the heart extended from the level of T3 to the level of T8 and its long axis (black line) was tilted moderately cranially. With 105 days (B), the heart extended from T2 to T7 with a much less pronounced cranial tilt. Cranial is to the left, caudal to the right. 1: aorta, 2: left ventricle, 3: right ventricle, 4: Truncus brachiocephalicus, 5: esophagus.

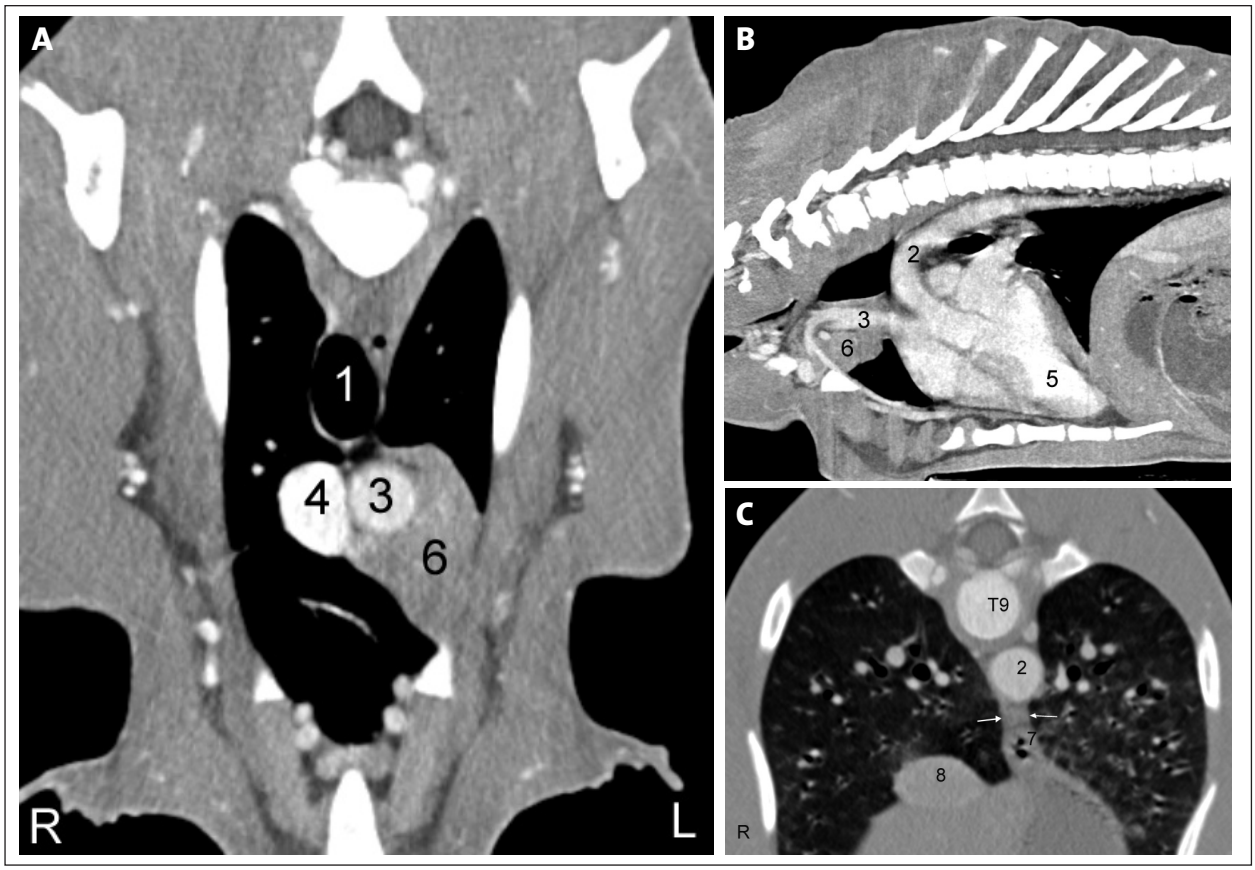

Figure 2: CT angiographic images of the unpaired left thoracic part of the thymus (A, B) and the caudal mediastinal lymph node (C) of a calf at the age of one day. In the transverse plane (A), the thymus was seen on the left side in the precardial mediastinum at all scans. In the sagittal plane (B), it appeared in all scans as a triangular to trapezoid structure lateroventral to the brachiocephalic trunk and to the left of the cranial vena cava. Cranial is to the left and caudal to the right (B). The caudal mediastinal lymph was always identified between the aorta and the esophagus just cranial to the diaphragm. 1: trachea, 2: aorta, 3: brachiocephalic trunk, 4: cranial vena cava, 5: left ventricle, 6: thymus, thoracic part, 7: esophagus, 8: caudal vena cava, arrows: caudal mediastinal lymph node.

ening (Fig. 3). Four calves had intralobular and interlobular septa formation, parenchymal bands, mosaic pattern, small nodules, consolidation of dorsal lung regions and mild thickening of the pleura (Fig. 3).

Discussion

This study measured various thoracic structures in young calves using computed tomography and was undertaken because of a lack of pertinent data in the veterinary literature. Certain relationships between various structures were calculated to control for weight and size differences among the calves. For instance, the ratio of the tracheal height to the thoracic height at the thoracic inlet did not change significantly during the study period and corresponded with normal values calculated in healthy non-brachiocephalic dogs (Harvey et al., 1982). Likewise, the ratio of the maximal height of the caudal vena cava to the length of the thoracic vertebra at the level of the bifurcation, and the ratio of the maximal height of the caudal vena cava to the maximal height of the aorta changed little after scan 2 and were similar to normal values in dogs. The ratios calculated at scan 1 were considerably greater than those at subsequent scans, possibly because of mild congestion of the caudal vena cava related to the transition from fetal to pulmonary circulation. Right heart insufficiency was ruled out by means of echocardiography.

The long axis of the heart changed with the growth of the calves from close to horizontal to more vertical, and the position of the heart moved cranially. A likely reason for this was the development of the forestomachs, primarily the rumen and reticulum, which caused the diaphragm to bulge cranially thereby displacing the heart as well. The vertebral heart score of the calves decreased on average by more than 1, presumably because the growth rate of the skeleton was higher than that of the internal organs. The vertebral heart score of 105-day-old calves was similar to the score in adult goats (Ohlerth et al., 2012). The vertebral heart score has been validated for the diagnosis of cardiomegaly in calves and a diagnostic cut-off value of 8.9 has been established for calves aged 25 ± 10 days (Suzuki et al., 2012). The dia-

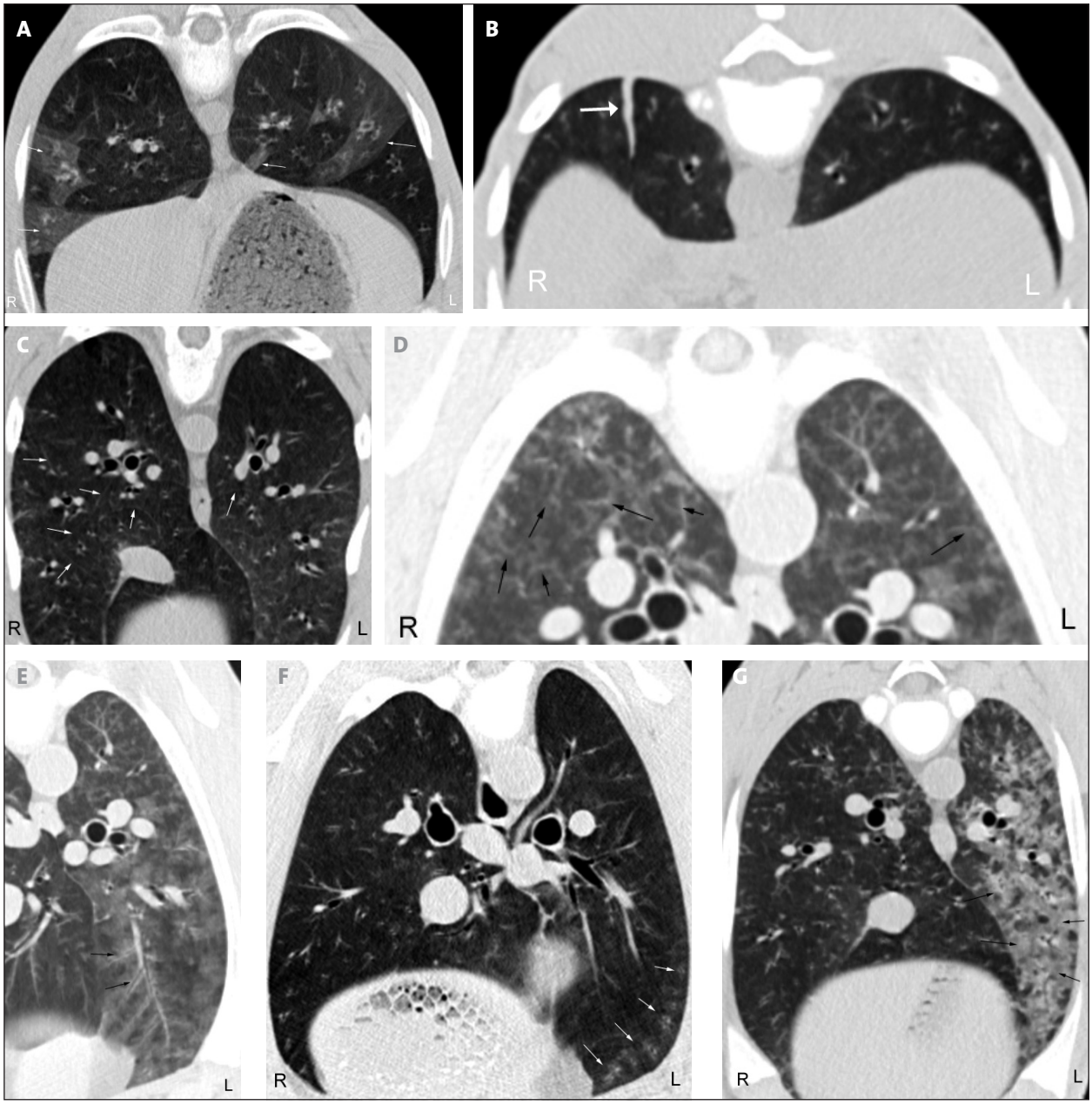

Figure 3: Transverse CT images (lung window) of lung changes seen in the caudal lung lobes of the study group: ground glass opacity (A), parenchymal bands (B), interlobular (C) and intralobular (D) septa formation, peribronchovascular thickening (E), bronchiectasis (F), and consolidation (G).

meter of the pulmonary blood vessels of the caudal lung lobes were significantly larger at scan 1 compared with scan 2, and this was also thought to be due to congestion attributable to protracted postnatal inflation of the lung associated with increased intrapulmonary pressure (Linke, 2009). It was unfortunate that 4 calves developed clinical bronchopneumonia during the study. This hampered the extrapolation of normal ranges from our observations but it closely reflected field conditions considering the high frequency of respiratory diseases in young calves (Rademacher, 2007). The lung changes seen on the CT images were similar to those reported in human patients with acute viral or bacterial pneumonia (Collins, 2001) and most likely reflected enzootic bronchopneumonia. This is a classical multifactorial disease causing outbreaks of febrile bronchitis, pneumonia and pleuritis in groups of housed calves. In addition to inanimate endogenous and exogenous factors that adversely affect the immune system, causative agents include viruses, bacteria, fungi and parasites (Dirksen et al., 2006). The recognition of very mild lung changes in CT images before 4 of the examined calves of the present study were overtly ill is of interest because it highlights the high sensitivity of the technique and may provide an early diagnosis and thus more effective treatment. However, clinicians should be aware of potential artifacts caused by patient positioning during scanning, such as atelectasis in

ventral lung regions caused by sternal recumbency, which was seen in our calves. It is possible that these lesions as well as ground glass opacities seen at the first scan immediately after birth were enhanced by incomplete inflation of the lung. Complete inflation of the lung may take up to two weeks and proceeds from cranial to caudal and from dorsal to ventral (Bostedt et al., 2009), which could explain why most of the lesions were seen in the ventral two thirds of the caudal lung lobes. The calves were considered healthy at scan 1 and an infectious cause for the lesions was therefore unlikely, notwithstanding a report that showed pathological lung changes on CT images 24 hours after experimental infection with *Mannheimia haemolytica* (Lubbers et al., 2007). The mean lung density of the calves was considerably higher than in people (–875 to –770 HU [Jacobi and Thalhammer, 2006]) or dogs (–854.55 to –830.75 HU [Morandi et al., 2003]) and was comparable with that of clinically healthy goats (Ohlerth et al., 2010). Because all calves developed pneumonia during the study, it is possible that some lymph nodes were reactive and therefore larger than normal.

Computed tomography is a very sensitive diagnostic tool, which allows the reliable assessment of thoracic lesions that generate nonspecific or negative radiographic findings (Prather et al., 2005). However, in large animal practice, the use of CT may be limited to valuable farm animals because of its expense. Size and body weight of calves undergoing CT examination must be carefully considered. In summary, the description of the cross-sectional anatomy of the thoracic structures in young calves, the calculated reference values for landmark structures and the classification of pathologic lung changes seen on CT scans in the present study provide a foundation for future studies of calves with pulmonary disease.

Tomodensitométrie du thorax de veaux de la naissance à l'âge de 105 jours

Dans ce travail, on a relevé les valeurs normales de tomodensitométrie pour les structures thoraciques de veaux. Six veaux holstein-friesian en bonne santé ont pour cela été examinés sous narcose à six reprises, de leur naissance à l'âge de 105 jours, au moyen d'un scanner multi-barrettes sous forme native et en angiographie. On a reconstruit des images avec une épaisseur de coupe de 1.5 mm. On a effectué à chaque fois des mesures absolues et relatives du cœur, de la trachée, de l'aorte thoracique, de la veine cave crâniale et caudale, des bronches principales, des bronches lobaires avec les rameaux des artères et des veines pulmonaires, des ganglions lymphatiques ainsi que de la densité pulmonaire. Tous les animaux ont été euthanasiés à l'issue du sixième examen et quatre d'entre eux ont été congelés pour permettre une comparaison entre les images obtenues et des coupes anatomiques. Durant l'étude, quatre veaux ont présenté de la toux et un écoulement nasal. La tomodensitométrie a permis de diagnostiquer une bronchopneumonie légère à moyenne ainsi qu'une pleurésie. Bien que les animaux aient, après traitement, complètement guéri, des modifications légères à moyennes des images tomodensitométriques ont persistés jusqu'à la fin de l'étude. Une légère bronchopneumonie a même été diagnostiquée chez les deux animaux ne présentant pas de symptômes cliniques.

La tomografia computerizzata del torace dei vitelli dalla nascita fino all'età di 105 giorni

In questo lavoro, sono stati raccolti via tomografia computerizzata (CT) i valori normali delle strutture toraciche nel vitello. Sei vitelli di razza Frisona Holstein clinicamente sani sono stati esaminati per 6 volte, sotto anestesia generale, dalla loro nascita fino all'età di 105 giorni, via tomografia computerizzata multislice e angiografia. Le immagini sono state ricostruite con uno spessore di 1.5 mm. Le misurazioni assolute e relative del cuore, della trachea, dell'aorta toracica, della vena cava craniale e caudale, dei bronchi principali, dei bronchi lobare caudali con i rami delle arterie e delle vene polmonari, dei linfonodi e della densità del polmone sono state eseguite puntualmente. Tutti gli animali sono stati eutanasiati in occasione dell'ultimo esame e 4 vitelli sono stati congelati per un'analisi comparativa delle immagini TC di sezioni anatomiche. Durante lo studio, 4 vitelli hanno sviluppato tosse e secrezioni nasali. Grazie alla CT è stata diagnosticata una da lieve a moderata polmonite bronchiale e pleurite. Sebbene gli animali si siano completamente ristabiliti dopo il trattamento, si sono riscontrate delle leggere a moderate modifiche della CT fino alla fine dello studio. Anche nei due animali clinicamente sani è stata diagnosticata dalla CT una lieve broncopolmonite.

References

Abé M.: Computertomographische Untersuchung des Thorax von Kälbern von der Geburt bis zum Alter von 105 Tagen. Dissertation, Universität Zürich, 2013.

Armbrust L., Biller D., Bamford A., Chun R., Garrett L., Sanderson M.: Comparison of three-view thoracic radiography and computed tomography for detection of pulmonary nodules in dogs with neoplasia. J. Am. Vet. Med. Assoc. 2012, 240: 1088–1094.

Bostedt H., Linke B., Sanftleben P., Flor J., Brunner R.: Zur postnatalen Lungenentwicklung beim bovinen Neonaten und deren Bedeutung für die Manifestation pulmonaler Affektionen. Tagungsbericht der DVG-Buiatrik-Tagung 2009, Berlin, 66–69.

Collins J.: CT signs and patterns of lung disease. Radiol. Clin. North. Am. 2001, 39: 1115–1135.

Dirksen G., Gründer H., Stöber M.: Krankheiten von Bronchen und Lunge. In: Innere Medizin und Chirurgie des Rindes. 5. Aufl., Hrsg. G. Dirksen, H.-D. Gründer, M. Stöber, Parey Buchverlag in MVS Medizinverlage, 2006: 295–344.

Harvey C., Fink E.: Tracheal diameter: Analysis of radiographic measurements in brachycephalic and non-brachycephalic dogs. J. Anim. Hosp. Assoc. 1982, 18: 570–576.

Jacobi V., Thalhammer A.: Grundmuster im CT der Lunge und ihre Differenzialdiagnose. Radiologie up2date 2006, 6: 311–334.

Johnson V., Ramsey I., Thompson H., Cave T., Barr F., Rudorf H., Williams A., Sullivan M.: Thoracic high-resolution computed tomography in the diagnosis of metastatic carcinoma. J. Small. Anim. Pract. 2004, 45: 134–143.

Johnson V., Corcoran B., Wotton P., Schwarz T., Sullivan M.: Thoracic high-resolution computed tomographic findings in dogs with canine idiopathic pulmonary fibrosis. J. Small. Anim. Pract. 2005, 46: 381–388.

Linke B.: Computertomographische Untersuchungen zur Erfassung der Lungenfunktion bei vitalen Kälbern in der frühen postnatalen Periode. Dissertation, Justus-Liebig-Universität Giessen, 2009.

Lubbers B., Apley M., Coetzee J., Mosier D., Biller D., Mason D., Henao-Guerrero P.: Use of computed tomography to evaluate pathologic changes in the lungs of calves with experimentally induced respiratory tract disease. Am. J. Vet. Res. 2007, 68: 1259–1264.

Makara M., Dennler M., Kuhn K., Kalchofner K., Kirchner P.: Effect of contrast medium injection duration on peak enhancement and time to peak enhancement of canine pulmonary arteries. Vet. Radiol. Ultrasound 2011, 52: 605–610.

Mclaughlin R., Tyler W., Canada R.: A study of the subgross pulmonary anatomy in various mammals. Am. J. Anat. 1961, 108: 149–165.

Morandi F., Mattoon J., Lakritz J., Turk J., Wisner E.: Correlation of helical and incremental high-resolution thin-section computed tomographic imaging with histomorphometric quantitative evaluation of lungs in dogs. Am. J. Vet. Res. 2003, 64: 935–944.

Ohlerth S., Becker-Birck M., Augsburger H., Jud R., Makara M., Braun U.: Computed tomography measurements of thoracic structures in 26 clinically normal goats. Res. Vet. Sci. 2012, 92: 7–12.

Prather A., Berry C., Thrall D.: Use of radiography in combination with computed tomography for the assessment of noncardiac thoracic disease in the dog and cat. Vet. Radiol. Ultrasound 2005, 46: 114–121.

Rademacher G.: Infektionskrankheiten. In: Kälberkrankheiten, Ursachen und Früherkennung, neue Wege für Vorbeugung und Behandlung. 3. Aufl., Hrsg. G. Rademacher, BLV Verlagsgesellschaft, 2007, 39–82.

Schummer A., Habermehl K.-H.: Herz. In: Lehrbuch der Anatomie der Haustiere, Band III, 3. Aufl., Hrsg. K.-H. Habermehl, B. Vollmerhaus, H. Wilkens, H. Waibl, Parey Buchverlag im Blackwell Wissenschaftsverlag, 1996, 17–73.

Suzuki K., Uchida E., Schober K., Niehaus A., Rings M., Lakritz J.: Cardiac troponin I in calves with congenital heart disease. J. Vet. Intern. Med. 2012, 26: 1056–1060.

Waibl H., Wilkens H.: Arterien. In: Lehrbuch der Anatomie der Haustiere, Band III, 3. Aufl., Hrsg. K.-H. Habermehl, B. Vollmerhaus, H. Wilkens, H. Waibl, Parey Verlag im Blackwell Wissenschaftsverlag, 1996 a, 74–182.

Waibl H., Wilkens H.: Venen. In: Lehrbuch der Anatomie der Haustiere, Band III, 3. Aufl., Hrsg. K.-H. Habermehl, B. Vollmerhaus, H. Wilkens, H. Waibl, Parey Verlag im Blackwell Wissenschaftsverlag, 1996 b, 189–275.

Corresponding author

PD Dr. med. vet. Stefanie Ohlerth
Section of Diagnostic Imaging
Vetsuisse Faculty, University of Zurich
Winterthurerstrasse 285c
8057 Zürich
Switzerland
sohlerth@vetclinics.uzh.ch

Received: 12 December 2013
Accepted: 19 March 2014